Sn Thin Film Deposition using a Hot Refractory Anode Vacuum Arc

I. I. Beilis, Y. Koulik and R. L. Boxman

Electrical Discharge and Plasma Laboratory, School of Electrical Engineering, Faculty of Engineering,

Tel Aviv University, P.O.B. 39040, Tel Aviv 69978, Israel, beilis@eng.tau.ac.il

***Abstract*- A Hot Refractory Anode Vacuum Arc (HRAVA) starts as cathodic arc, heating the anode and depositing on it cathode material. When the anode is hot, all deposited cathode material is re-evaporated from the anode forming cleaner radially expanding plasma. It was shown that the rate of deposition reached 2-3 μm/min with significantly reduced macroparticle contamination in Sn films produced by HRAVA with current *I*=60–175 A and duration up to 180 s.**

I. INTRODUCTION

Sn thin film deposition is important in coating applications. Bimetallic Cu-Sn thin films are use in bonding components in many electrical and electronic devices to Cu conductors [1]. Bimetallic Cu-Sn thin films were prepared by consecutively depositing 560 nm of Cu and either 200 or 500 nm of Sn by e-beam evaporation onto 2.54 cm diameter fused quartz disks at a rate of ~0.5 nm/s [1]. Electroplating was used to deposit thin Sn films on copper substrates [2]. Sn thin films are needed for the anode layer of thin film Li-ion batteries due to its higher Li storage capacity in comparison than graphite anodes. Nimisha *et al* [3] fabricated Sn thin films by rf sputtering. The substrate to target distance was maintained at 5 cm with a deposition rate of 1 nm/s. Traditional deposition techniques, such as chemical vapor deposition (CVD), or pulsed laser deposition (PLD) are costly and have low-throughput.

The conventional vacuum arc plasma jet is also used for depositing coatings [4] which is related to the physical vapor deposition (PVD) techniques. The main problem with it is the generation of macroparticles (MPs) at the cathode. The Hot Refractory Anode Vacuum Arc (HRAVA) was proposed in last decade as a thin film deposition technique which produces MP-free coatings [5]. The HRAVA initially operates as a conventional cathodic vacuum arc and the cathode spot plasma jets deposit cathode material, including MPs, on a refractory anode surface while simultaneously heating the anode. When the anode reaches a sufficiently high temperature (~2000K) the previous coating and impinging cathode material from the plasma jets are re-evaporated or reflected from the hot anode. Also MPs are evaporated in the inter-electrode gap plasma. The HRAVA forms MP-free anode plasma which expands radially and can be used for depositing metallic coatings [5].

The HRAVA phenomena and deposition characteristics were investigated previously for thin film materials such Cu, Ti, Cr, Al and Zn [6,7]. Deposition rates of 1-3 μm/min were obtained with arc current in the 150-300A range.

However Sn deposition was only tested briefly [7] demonstrating relatively large rate of deposition. The details of very low melting Sn film characteristic were not investigated previously. The objective of the present work is to explicit the Sn film time evolution thickness, rate of deposition and MP contamination for different arc currents.

II. EXPERIMENTAL SETUP

Vacuum Chamber and Electrodes. A cylindrical vacuum chamber (400 mm length, 160 mm diameter), as shown schematically in **Fig. 1** was used for the experiments. The chamber was evacuated by an oil diffusion pump to 1.3×10^{-2} Pa.

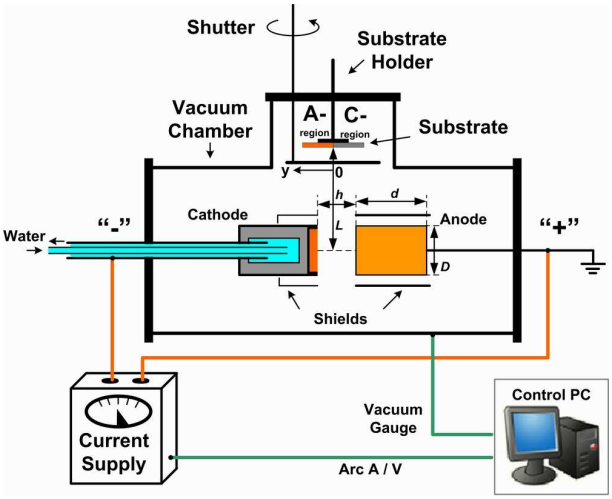

Fig. 1. Schematic diagram of the chamber, cathode-anode assembly and the substrate position with A and C regions.

During the arc, the pressure in the chamber was 5.3×10^{-2} Pa. The arc was sustained between a water-cooled Cu cup cathode filled with Sn, and a non-consumable cylindrical anode, for time

periods up to 180 s, operating with a current I=60-175 A. The Sn cathodes had a D=30 or 60 mm diameter and d=10 mm thickness.

The 30 mm diameter cathode was used with two graphite anodes, with d=9, 15 mm and D=32 mm and with gap h=10 mm. The 60 mm cathode was used with a W anode with d=10 mm, D=60 mm and h=10 and 15 mm. A D=70 mm stainless steel cylindrical radiation shield surrounded the graphite anode to reduce radiative heat loss during deposition. The W anode was used without a radiation shield. The anodes were supported by a thin tungsten rod that also connected it to the electrical circuit. The D=30 mm cathode was surrounded by a square boron nitride box-shaped shield with 65 mm sides; the cathode was recessed 3 mm behind the shield. The D=60 mm cathode was used with the boron nitride flat plte shield positioned between cathode and substrate and the cathode recessed 7 or 10 mm behind the shield for the h=15 mm case, while for the h=10 mm case no cathode shield used. The purpose of above shields was to block MP flux originating at the cathode from reaching a portion of substrate, designated the *A-region* (**Fig. 1**, see also below). The arc current was supplied by a welding power supply (Miller XMT-400 CC/CV). The anode was grounded and the chamber was floating.

Substrate preparation. The substrates were 75x25 mm glass microscope slides. The substrates were pre-cleaned by liquid detergent and water, and were then soaked in alcohol. A substrate was mounted on a holder which was movable in the radial direction, and was positioned at a distances of L=110 and 125 mm from the electrode axis (95 mm from cathode edge), facing the plasma flux emanating from the inter-electrode gap. The holder was separated from the arc plasma by a shutter which controlled the deposition onset and duration (15 s).

Coating characterization. As observed previously [5,6] the cathode shield position determined the location of a boundary between regions on the substrate with low and high MP contamination, designated as the anodic (*A*) and cathodic (*C*) regions, respectively (**Fig. 1**) [6]. The *C-region* faced the cathode and contained MPs emitted from the spots. The *A-region* faced the anode and collected anode plasma that was almost free of MPs. The MPs and deposited films in the *A-region* (about 3-5 mm from the *A-C* boundary) were characterized. The MPs were counted using an optical microscope and a digital camera, which could detect MP's larger than approximately 1-3 µm. The MP density was determined by counting the number of MPs per mm^2. The thickness was measured by profilometry of films deposited on substrates exposed to the plasma for 15 s when the shutter was open, beginning at various times from arc ignition. The deposition rate (V_{dep}) was determined as the ratio of the film thickness on the glass substrate to the exposure time. The cathode erosion rate was measured by weighing the cathode before and after arcing.

III. RESULTS AND DISCUSSION

A. Deposition Rate

Fig. 2 presents the measured Sn deposition rate dependence on time beginning from arc ignition, with I as a parameter, using a D=60 mm cathode, W anode, h=10 mm and without a cathode shield. It can be seen that V_{dep} increased with time in studied range of all arc currents. For I<100 A the V_{dep} increase was very weak, while for larger arc currents the V_{dep} increase was very significant.

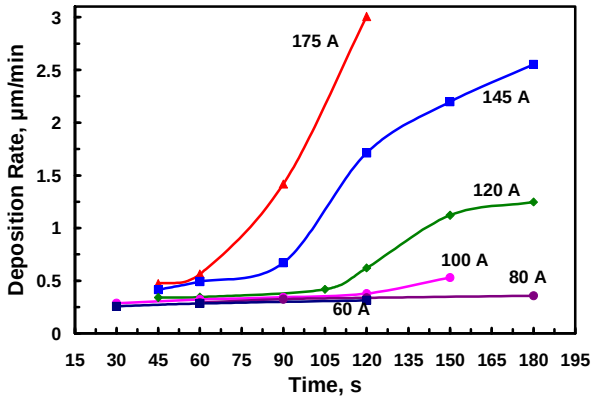

Fig. 2. Time-dependent rate of Sn film deposition, D=60 mm cathode without shield, d=10 mm W anode, h=10 mm, L=125 mm.

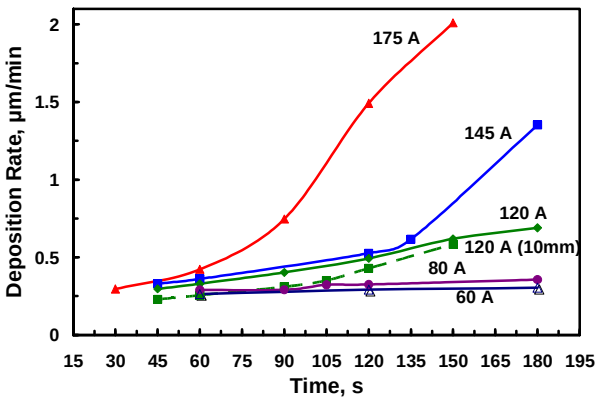

Fig. 3. Time-dependent rate of Sn film deposition, D=60 mm cathode recessed 7 mm behind shield, d=10 mm W anode, h=15 mm, L=125 mm. (The cathode recessed 10 mm behind the shield is also shown for I=120 A).

Thus, V_{dep} increased from 0.5 to 3 µm/min when the arc time increased from 45 to 105 s for I=175 A, while for I=80 A the V_{dep} was approximately constant in time.

The time dependent deposition rate for a

D=60 mm cathode with a BN cathode shield protruding for 7 mm above the cathode, W anode, and *h*=15 mm is presented in **Fig. 3**. In this case V_{dep} also increased for all investigated *I* but was lower than in the previous case without a cathode shield (V_{dep} increased from 0.3 to 2 μm/min for *I*=175 A). The case with the cathode shield protruding 10 mm above the cathode is also shown in **Fig. 3** for *I*=120 A and the deposition rate was slightly lower than for the case with the shield protruding 7 mm (~0.58 and ~0.62 μm/min respectively at 150 s).

The time dependent deposition rates for a *D*=30 mm cathode and *d*=9 and 15 mm graphite anodes are presented in **Figs. 4** and **5** respectively.

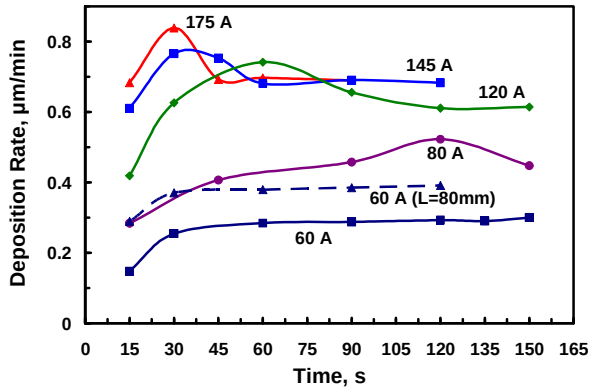

Fig. 4. Time-dependent rate of Sn film deposition, *D*=30 mm cathode recessed 3 mm behind box shield, *d*=9 mm graphite anode, *h*=10 mm, *L*=110 mm. (The case for *L*=80 mm is also shown for *I*=60 A).

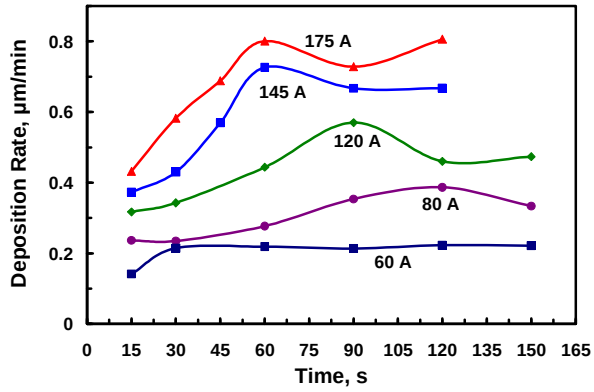

Fig. 5. Time-dependent rate of Sn film deposition, *D*=30 mm cathode recessed 3 mm behind box shield, *d*=15 mm graphite anode, *h*=10 mm, *L*=110 mm.

The BN cathode shield protruded 3 mm above the cathode and *h*=10 mm. It can be seen that V_{dep} increased with time to a peak (for *I*>80 A), and then decreased to a steady-state value. The peak value depended on the current (with *d*=9 mm, 0.74 and 0.84 μm/min for *I*=120 and 175 A respectively,) and the peak time decreased with *I* (from 60 to 30 s for *I*=120 and 175 A respectively, *d*=9 mm). At steady state with *d*=9 mm, V_{dep} increased from 0.3 to 0.7 μm/min with increasing arc current from 60 to 175 A respectively. The deposition rate for the thicker anode (*d*=15 mm) had peaks for same arc currents (**Fig. 5**) but the peaks occurred much later (90 and 60 s for *I*=120 and 175 A respectively) and the peak was wider than with the *d*=9 mm anode.

Also V_{dep} at the peak for *d*=15 mm was lower than with the *d*=9 mm anode (0.57 and 0.80 μm/min for *I*=120 and 175 A respectively, *d*=15 mm).

A V_{dep} peak was not observed with *D*=60 mm for all arc currents and was observed for smaller *D*=30 mm cathode only for *I*>80 A. Its value increased with *I* and the time appearance depended on *d*.

The observed effects can be understood, firstly, taking into account that in the HRAVA the anode heating decreased with *d* and increases with *I* [8]. Secondly, the relatively large MP production from Sn cathode spots should be noted. The measured total cathode erosion rate for Sn (~300 μg/C) with *I*=100 A, where the main part of the Sn erosion was in MP form (~200 μg/C) [4].

The reason for the peak in V_{dep} is the initial condensation of large amounts of MPs and cathode plasma on the cold anode surface. During arcing the anode is heated, and the condensed material (including MPs) was evaporated from the anode when it reached an appropriate temperature.

During the V_{dep} peak, the rate of deposition was determined by the vapor produced by the cathode spots plus the vapor generated by the evaporation of previously condensed MPs and plasma reaching the anode. Later, when the anode was sufficiently hot, and all of the condensed material on the anode completely evaporated, the lower steady state level of V_{dep} was determined by the cathode plasma jets products re-evaporated and reflected from the hot anode.

The rate of anode temperature increasing influences the rate of material evaporation from the anode. For relatively large *I* and small *D* the anode was quickly heated and therefore the vaporization was contributed stronger quickly increasing in time the anode plasma density in time and as result the V_{dep} peak appeared.

In contrast, for small *I* and large *D* the anode heating rate is weaker and therefore V_{dep} increased monotonically. As the transitory heating time is larger using thicker anodes, the V_{dep} peak for *d*=15 mm appeared later than for *d*=9 mm. Thus this result indicates when the steady-state process appeared that preferable using for engineer applications.

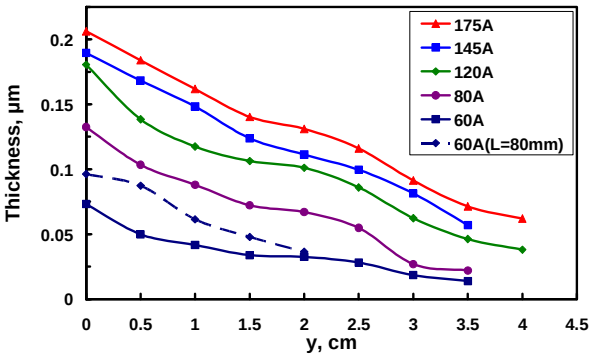

Fig. 6. Sn film thickness distribution in the A-region of the substrate in the y-direction from the A–C boundary with arc current *I* as a parameter. *D*=30 mm cathode recessed 3 mm behind box shield, *d*=9 mm graphite anode, *h*=10 mm, *L*=110 mm. (The case for *L*=80 mm is also shown for *I*=60 A).

B. Film Thickness Distribution

Fig. 6 shows the Sn film thickness distribution on the substrate in *y-direction* (parallel with the electrode axis - see **Fig. 1**), in the *A-region* (y=0 is at the *A-C boundary*) with arc current as parameter. It can be seen that the film thickness decreased with *y* in the measured range of *I* and it reached about half at *y*=2-3 cm, depending on *I*. The thickness increased with *I* relatively weaker from 120 to175 A than from 60 to 120 A.

C. MP Contamination

The MP density as a function of *I* is presented in **Fig. 7** for Sn (60 and 30 mm diameter cathodes). For comparison previously measured MP density for Al, Zn, Cu, Cr cathodes [6,9] are also presented. The substrates were exposed for 15 s after 60 s of arcing, *L*=110 mm, *h*=10 mm. The MP density for Sn is larger than for other volatile materials like Al, Zn, and increases with *I* up to 80 A, and then decreased with further increasing of *I*. The MP density for intermediate materials like Cu, Cr was significantly lower than for Sn.

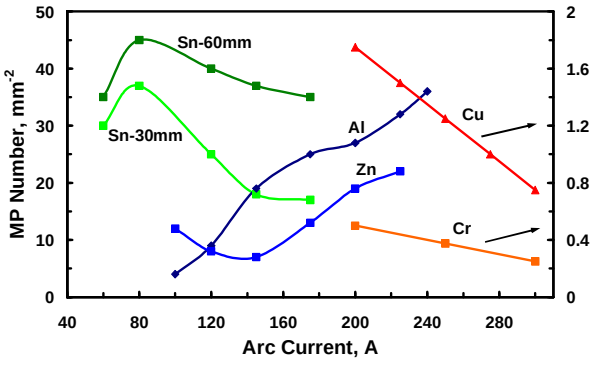

Fig. 7. Dependence of MP density on arc current for Sn (measured here), Zn and Al (left axis) and for Cu, Cr (right axis) [6,9], recessed cathodes. The substrate was exposed after 60 s for 15 s, *L*=110 mm.

Due to large difference between the very low Sn melting temperature (T_m=232C) and relatively large Sn boiling point (T_b=2687C) there is a relatively large MP fraction in the Sn cathode erosion. This fact explains the large MP contamination detected in Sn films, compared to Cu, Ti, and also to Al, Zn (I<150 A) for which the difference between T_m and T_b is significantly lower [9].

IV. CONCLUSIONS

1. Sn films were successfully deposited on glass substrates using HRAVA with different electrode geometries and currents.

2. V_{dep}(t) had a peak with a *D*=30 mm electrode pair and *I*>80 A, while for *D*=60 mm electrode pairs $V_{dep}(t)$ was monotonic. The peak was higher at higher current. For thicker anodes, the peak appeared at later times.

3. V_{dep} is significantly larger for larger *D* when *I*≥120 A (see Fig2 and Fig.4), due to stronger evaporation of the MPs at relatively high *I*. For this case, MP contamination decreased with *I*. Thus, V_{dep} with *D*=60 mm electrodes exceeded this rate for *D*=30 mm electrodes by a factor 2.5 (*I*=145 A, 120s, see Fig2 and Fig.4).

REFERENCES

[1] K.N. Tu and R.D. Thompson, Acta metall., **30** (1982). 947.

[2] M. Inaba, T. Uno, A. Tasaka, Journal of Power Sources **146** (2005) 473.

[3] C.S. Nimisha, G. Venkatesh, K. Yellareswara Rao, G. Mohan Rao, N. Munichandraiah, Materials Research Bulletin **47** (2012) 1950.

[4] Handbook of Vacuum Arc Science and Technology. edited by R.L. Boxman, P. Martin, D. Sanders (Noyes Publishing, Ridge Park NJ, 1995).

[5] I.I. Beilis, S. Goldsmith, R.L. Boxman, Surf. Coat. Technol., **91** (2000) 133-134.

[6] I.I. Beilis, R.L Boxman, Surf. Coat. Technol., **204** (2009), 865.

[7] I.I. Beilis, Y. Koulik, R.L. Boxman and D. Arbilly, J Mater Sci, **45** (N23) (2010) 6325.

[8] I.I. Beilis, Y. Koulik, R.L. Boxman, IEEE Trans. Plasma Sci., **39** (N6, Part 1) (2011) 1303.

[9] I.I. Beilis, Y. Koulik, R.L. Boxman and D. Arbilly, Surf. Coat. Technol., **205** (2010) 2369.